SOME REGULARITIES IN VARIATIONS OF THE MICROSTRUCTURE PARAMETERS OF TRANSLUCENT CLOUDS

A.A. Isakov

Institute for Atmospheric Physics,
Russian Academy of Sciences, Moscow
Received August 12, 1998

We analyze the phase functions of the sun aureole brightness in translucent clouds measured during the complex cloud experiment in the fall of 1996 in the Moscow region. The particle size-distributions $V(r)/dr$ measured in cirrus are shown to be very stable, regardless of the optical depth and cloud form, both in shape and position of the maximum (radii of optically equivalent spheres $R = 22 - 25$ μm). As a result, the cloud optical depth τ and the total volume of particles V_Σ turn out to be related linearly, with the effective radii of particles R_{ef} varying only slightly about the value of 35 μm. In altocumulus, the particle size distribution may be very stable within one cloud formation, while changing noticeably from case to case (the characteristic size is 3–5 μm). In cirro-cumulus q c the particle size is even smaller – 1.5–3 μm and may change during several minutes. In the contrails living for about one hour, the mode of relatively large particles with the radius about 10 μm is formed.

INTRODUCTION

This paper presents some results of investigation of the translucent clouds with a sun aureole photometer (hereinafter, SAPh). The investigations have been carried out during the complex cloud experiment (September–October period of 1996) at the Zvenigorod scientific station of the Institute for Atmospheric Physics of the Russian Academy of Sciences. The SAPh used had been designed for studying the coarse-disperse aerosol in the atmospheric column. In our previous atmospheric experiments in 1992–1994 it was used practically without any adaptation to the new object under study. On the basis of new experience gained from the photometer operation, the main items of its desirable modification to meet the requirements of cloud studies have been formulated in Refs. 1 and 2. Those include a significant (by several times) decrease in time needed to record the angular patterns (the spectral ones being recorded during about 1 s) of the aureole brightness phase function $\mu(\varphi, \lambda)$ and the capability of making measurements at as minimum scattering angles φ as possible. The first requirement is caused by the necessity to minimize the influence of the spatiotemporal inhomogeneity of cloudiness thus providing the possibility of detecting variations of the optical properties of the translucent clouds. The second requirement must provide for diagnostics of gigantic, with the equivalent radius up to $r \sim 40–50$ μm, particles of cirrus.

Reference 2 introduces the angular instrumental function $A(\varphi - \varphi_0)$, which allows for the finiteness of the angular size of the sun and the photometer field of view. As a result, the recorded brightness phase function $\mu(\varphi)$ is related to an actual one, $\mu^*(\varepsilon)$, by the following equation:

$$\mu(\varphi) = \int A(\varphi - \varepsilon)\, \mu^*(\varepsilon)\, d\varepsilon. \qquad (1)$$

Analysis of calculated $A(\varphi - \varepsilon)$ has shown that the range of angles can be expanded to $\varphi = 1°$. The measurement errors associated with its nonideal shape do not exceed 5% in this case.

MEASUREMENT TECHNIQUE AND INSTRUMENTATION

The SAPh modification consisted in the following.

1. The disk-modulator with six optical filters was added to the device. Thus, the formerly available set of the operating wavelengths ($\lambda = 0.46$, 0.54, 1.2, and 1.55 μm) was supplemented with $\lambda = 0.62$ and 0.82 μm by adding two new filters.

2. A new automated scanner was been designed and manufactured to provide the set of measurement angles $\varphi_i = 1.2$, 1.6, and 2.2 under cloudy sky conditions and $\varphi_i = 1.6$, 2.2, 4.4, 6.6, and 8.8 for the case of clear skies. A brief explanation is needed here. The level of illumination was estimated to be several tenths of sr^{-1} at $\varphi = 1.2°$ and the atmospheric mass $m \sim 2$. Even for thin, with $\tau \sim 0.1$, cirrus clouds, it makes only several percent of the μ value. At the same time, the error may reach several tens of percent when recording the brightness phase function of the clear

0235-6880/98/12 1117-06 $02.00

sky. That is why the angle $\varphi = 1.2°$ was excluded from the second set of angles.

The operation of SAPh itself and the procedure of signal recording are almost completely computer-controlled. This allows a reduction of time needed to record the cloud phase functions to about 10 s as short. The complete cycle of measurements (i.e., recording of zeros and signals, scanner reset, etc.) takes about 1.5 minutes.

That short recording time (during 10 s the sun moves along the azimuth by about 2 minutes of arc) enabled us to replace the tracking system, ***when studying translucent clouds***, by an "optical sight" providing for about 2-minute of arc reproducibility of aiming at the sun. After completion of the preliminary cycle, the device is aimed at the sun, and the direct solar flux and $\mu(\varphi)$ at three scattering angles are recorded during 10 s.

The set of scattering angles $\{\varphi_i\}$ determines the linear dimensions of the cloud volume contributing to of the brightness phase function recorded besides the measurement time. Naturally, the smaller are these dimensions, the less strict restrictions are imposed upon the inhomogeneities of the cloudiness field under study. Consequently, the cloudiness spatiotemporal inhomogeneity itself can easily be transformed into the object for a study. Dimensionality of the vector of measurements μ_k, i.e., the number $n = i \times j$ of all measured parameters $\mu(\varphi_i, \lambda_j)$, must provide for stability of the inverse problem solution. Three angles give $n = 18$, and, as analysis shows, that is enough.

Based on the conclusions drawn from the mathematical experiment in Ref. 2, we have chosen $r = 80$ μm as the upper boundary for the kernel of the inverse problem equation when transformed to the algebraic form.

MEASUREMENT CONDITIONS

In this year dry and sunny weather was observed in Moscow region in the second decade of September and until the end of October. Therefore, the observations with the SAPh continued even after termination (October 5) of the complex experiment. This period included twenty days of observation; two of them were cloudless, while on other days almost all types of translucent clouds listed in the Album of Clouds (Ref. 3) occurred.

Clouds were identified visually according to the Album, because the cloud height meters used in the experiment are incapable of detecting the height of thin clouds boundary. Most often different types of cirrus were observed, and the cases of two-layer cloudiness *Ci* + *Ci* were also detected occasionally. Cumulus clouds were mainly observed as *Cc* or *Ac* in combination with the upper *Ci* layer. Only once the *Ac* clouds were observed as a vast even field with the characteristic angular dimensions of "fleecy clouds" about 1°. In the majority of cases either separate *Ac* fields with dimensions about tens of kilometers or *Cc* areas on the periphery of cirrus fields prevailed. It is worth noting that the cirrus structure kept almost constant with time, while transformation processes in *Cc* could be observed even visually. The characteristic time of transformation was about several minutes, so that sometimes clouds thickened or dissipated even while being seen.

The short time of recording has allowed these variations to be followed up in a number of cases (see below). However, the number of records made for *Cc* and *Ac* were significantly fewer than for *Ci* and *Cs*. The total number of records exceeded two hundreds, about 10% of records were rejected for the reasons of cloudiness inhomogeneity. The total number of cases (by a case is meant the recording of no less than three–five records for one cloud formation, single records were done only for the contrails) is presented in the Table I along with the distribution of cases over cloud type. When analyzing the Table, one should keep in mind that both *Cs* and *Ac* were sometimes observed during same day.

TABLE I.

Type of the case	Clear sky	*Ci*	*Ci* + *As*	*Ci* + *Ci*	*Ci* + *Cc*	*Ci* + *Ac*	*Cc*	*Ac*	Contrails
The number	12	12	2	2	3	5	2	5	8

The particular emphasis should be given to two days — September 30 and October 12. The first case corresponds to the scheme of atmospheric front passage described in Ref. 3. In the morning, around 09:00 a.m., thin even cirrus clouds were observed, then the cloudiness became a two-layer *Ci* + *Ci*. At about 11:30 a.m. wide and even *Ci* spissatus jets appeared. They came from west-south-west and gradually became more dense. At about 02:30 p.m. they gave way to even cirrostratus *Cs*.

At 04:30 p.m. the dense altostratus, *As*, clouds were observed, and in the evening they were replaced by *Ns*.

The period, most convenient for measurements, lasted about three hours, during which we succeeded to follow up the dynamics of optical characteristics of cirrus clouds with their optical depth varying as $\tau \approx 0.1–1.5$ (see below). About 30 records were recorded during these three hours.

The case observed on October 12 is schematically similar to the first one (including the chronology), but it was preceded by the trailing edge of the cold atmospheric front – in days preceding this event it was cloudy and rainy, and the pressure "ridge" was observed in the evening before this day. Thin cirrus clouds coming from south-west gave way to more dense

Ci spissatus jets, and at about 02:30 p.m. the even *Cs* field with the distinct boundary was observed, at about 04:30 p.m. it transformed into the *As* field. About 50 records have been taken that day with the depth varying from $\tau \approx 0.1$ to 1.3. Note that in the above-described cases such rather rarely occurring optical effects were observed as the double halo and the rainbow arcs, what indicates that the ice crystals had a preferred orientation (ordered in space).

The contrails have been detected eight times during the experiment, and in two cases they were observed against the background of thin cirrus clouds. All the contrails observed could be considered as old ones, because they were observed about half an hour and after the aircraft had flown off.

Prior to analysis of the measurement results, let us return to the problem of multiply scattered radiation. In Ref. 4 the contribution coming from multiple scattering has been estimated in the small-angle scattering approximation. As follows from the figure presented in Ref. 4, if the optical depth of a layer is $\tau \approx 1$, this contribution is less than 10% and ***almost independent of an angle*** within the scattering angles $\varphi = 1 - 2°$. Otherwise it only changes the level of $\mu(\varphi)$, while keeping unchanged its angular behavior. Similar estimates may be found in Ref. 5. This circumstance has also been taken into account when choosing the set of $\{\varphi_i\}$ angles. The narrow width of aureole in cirrus leads, as known, to underestimation of their optical depth as measured for the direct solar radiation.[6] Besides, in the optical depth of most thin *Ci* clouds, cannot be separated from τ of the atmospheric aerosol, which almost always exceeds 0.1. For this reason we used in our analysis the optical depths calculated based on the reconstructed size-distributions of the ensembles of cloud particles.

DISCUSSION

As was noted above, the majority of records were obtained for different types of cirrus: fibrous, edge-shaped, tangled, cirrostratus (fibrous and fog-like), etc. Such a variety of shapes seems to correspond to the variety of optical and microphysical characteristics of clouds. However, analysis of the results obtained from inverting about 150 phase functions recorded in ten cases that made the main bulk of observations led us to an unexpected conclusion that particles of cirrus clouds in the size range $r = 0.3–50$ μm show the distribution of their volume over size to be stable in shape and the position of maximum ($r \approx 22–25$ μm) ***irrespective of the subtype of clouds and cloud optical depth***. The rms errors, μ, of the reconstruction are about 5–10%. One of the causes of such a stability of $dV(r)/dr$, as compared to a droplet cloud, is quite obvious – the ice particles are insensitive to pulsations of the relative air humidity. However, this cause does not explain the reproducibility of the results. This is illustrated by Fig. 1*a*.

Figure 1*a* presents three curves $dV(r)/dr$ for two different days: September 30 and October 5. Curves *1* and *2* (the left ordinate axis) correspond to close ($\tau = 0.95$ and 0.82) optical depths but on different days. Curve *3* (the right axis) was obtained in the same day as curve *2*, but with a four times lower ($\tau = 0.22$) optical depth. The distributions are rather narrow – their halfwidths are $\Delta r / r_{max} \sim 0.3$. It was noted in Ref. 2 that the algorithm for solution of the inverse problem has certain drawbacks. In order to exclude their manifestations, we have analyzed the initial data – scattering phase functions $\mu(\varphi, \lambda)$. For every case, we have calculated the regressions $\ln \mu(\varphi = \text{const}, \lambda)$ of $\ln\lambda$ at three scattering angles φ for six wavelengths. These relationships approximate the spectral dependence of the phase functions. It turned out that ***all over the data array*** 1) there exists a linear relation between these parameters with less than 5-% deviations of experimental points from the regression straight line; 2) the angular coefficients K of the straight-line regressions for $\varphi = 1°$ have very small spread in values (Fig. 2, the left ordinate) and the value $K_1 \approx 1.2$, almost ***independent of the cloud optical depth*** τ (the abscissa), for $\varphi = 2.2°$ $K_3 = 1.0$ ($K_2 = 1$ certainly occupies the intermediate position, but it is not shown in the figure in order to make it more clear). The spread of K_3 for the smallest optical depths is associated with the contribution from the coarse-disperse atmospheric aerosol, for which the spectral dependence of the phase function differs from that for a cloud. So, first, the stability of the reconstructed distributions $dV(r)/dr$ results from the very high reproducibility of the spectral and angular dependence of brightness of the aureole produced by different types of cirrus clouds. This stability is not a result of peculiarities of the algorithm of the inverse problem solution. Second, with the optical depth varying as $\tau \approx 0.2–1.5$ distortions of the spectral and angular dependence (rather than the general level) due to multiply scattered radiation most likely do not exceed 5%.

In Ref. 2, it was noted that in cirrus the angular size of the visible aureole around the moon may vary by two to three times. At the first sight, this statement disagrees with the conclusion drawn above. In Fig. 1*a*, to the right from the main distribution bell around $r \approx 40 - 50$ μm one can see the second bell, which is several times smaller in magnitude. The validity of the parameters (markedly varying) of this mode is certainly lower than in the main mode. However, it is just the particles of the second mode that apparently determine variations of the visually observed aureole peak of μ, while this peak (for clouds of the *Ci* type) is beyond the range of operation angles.

Such a parameter as the effective radius of particles R_{ef} is often used in theoretical calculations for parameterization of the cloudiness characteristics. This parameter is equal to the ratio of the total volume of particles to their total area of cross sections. We have also calculated this parameter (certainly, for the size range $r = 0.5 - 80$ μm) for the whole data array. As the coefficient K (and by the same reason), the effective radius R_{ef} has a small spread in values and only at $\tau \le 0.2$. For large depths it stabilizes at the value $R_{ef} = 35 \pm 1$ (Fig. 3, the left axis).

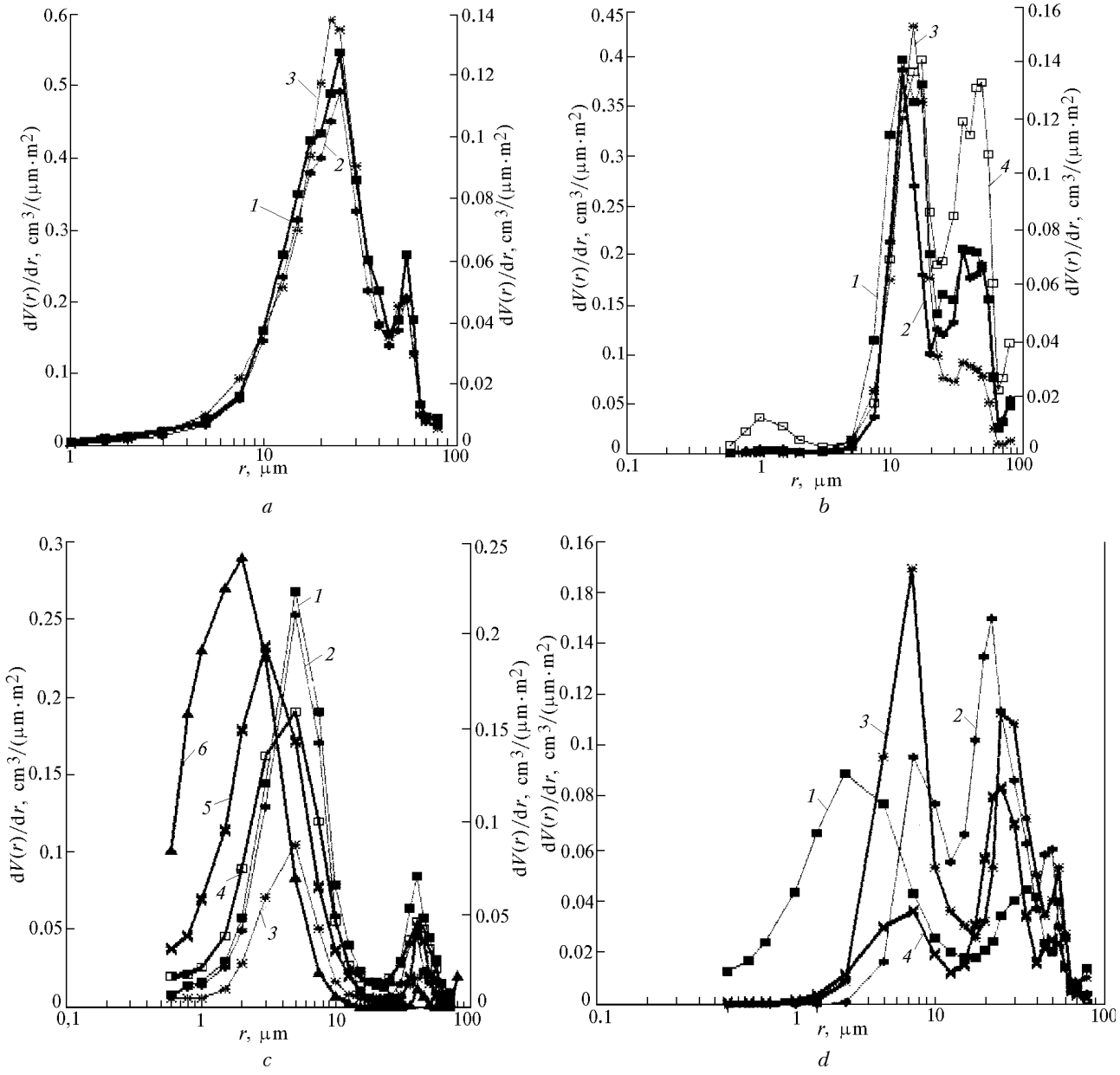

FIG. 1. Particle size-distribution for three cases of cirrostratus Cs : (a) October 5, $\tau = 0.95$ *(curve 1) September 30,* $\tau = 0.82$ *and* 0.22 *(curves 2 and 3, respectively); (b) September 25, a separate cirrus cloud, the recording time* 04:14 p.m. *(curve 1),* 04:18 p.m. *(curve 2),* 04:23 p.m. *(curve 3), and* 04:27 p.m. *(curve 4); (c) altocumulus Ac field (the left axis, curves 1–3, the interval between records was about* 5 min*) and cirrocumulus Cc (the right axis, curves 4–6, the interval about* 2 min*); (d) "old" (with the age about half an hour and more) contrails.*

These Figures also show the dependence of the total volume of particles V_Σ (the right axis) calculated from the $dV(r)/dr$ curves in the range $r = 0.3$–80 μm on the reconstructed optical depth τ. The straight line on the figures corresponds to $V_\Sigma = 16\tau$, V_Σ in cm^3/m^2. The linear relation between the parameters proportional to the cubed radius of particles (V_Σ) and the squared radius (τ), which is illustrated by Figs. 2 and 3, is possible only at constant particle size distribution. The variations of V_Σ and τ are determined by the total number of particles in the column N. Most likely, this is the dependence on the geometrical thickness of a cloud (in meters), although variations of the particle number density at a steady state particle size distribution cannot be excluded. The coefficient of proportionality between the volume of particles and the cloud depth was calculated separately for three data sub-arrays: the data recorded on September 30, the data recorded on October 12, and all the remaining data. It turned out to be $\xi = 16$ accurate to ≈ 3% for all the three cases.

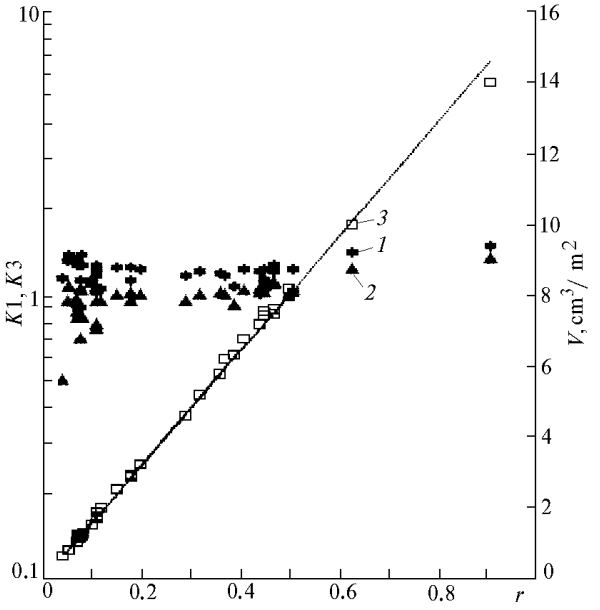

FIG. 2. The spectral dependence $K = d(\ln \mu)/d\lambda$ *of the aureole brightness for the scattering angles* $\varphi = 1$ *and 2 (1 and 2) and the total volume of particles* V_Σ *(3, the right ordinate axis) versus the optical depth* τ *of cirrostratus Cs. The straight line corresponds to* $V_\Sigma = 16\tau$.

Reference 7 presents some results of a study of cirrus clouds and contrails using from two airborne laboratories. Among other characteristics, the average values of the effective radius and the ice content for 1 m^3 of air are presented there. The cloud layer thickness is estimated in Ref. 7 to be approximately 1 km, therefore the conversion of IWC (ice water content) into the ice content in the column gave the value 20–50 g/m^3, which is not too different from the values presented in Figs. 2 and 3. The values of the effective radius also agree rather well ($R_{ef} = 26 - 30$ by the data from Ref. 7), taking into account the size range covered in measurements conducted in Ref. 7 and somewhat different equation for its estimation used.

The only case dropping out from the described scheme was recorded on September 25. The corresponding distribution curves $dV(r)/dr$ are presented in Fig. 1*b*. The main distribution mode here corresponds to significantly smaller size of particles and varies with time in the size range $r = 7$–15 μm (in the cloud experiment of 1994, one similar case was also fixed,[2] while all the rest cases correspond well to the above scheme.) The form and dynamics of the distributions, resemble the situation with contrails (see below), although the cloud was identified as cirrus. Maybe this was the initial stage of cirrus formation – in all other cases, clouds appeared near the horizon several hours before the time of recording.

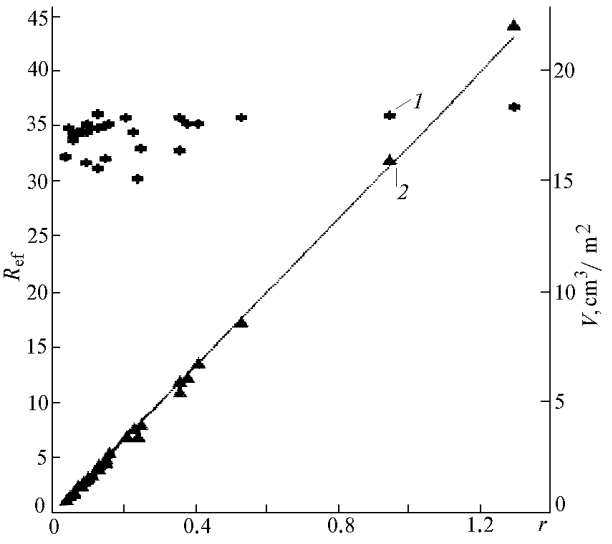

FIG. 3. The effective radius of particles R_{ef} *(1) and the total volume of particles* V_Σ *(2, the right ordinate axis) versus the optical depth* τ *of cirrostratus Cs clouds. The straight line corresponds to* $V_\Sigma = 16\tau$.

Cumulus clouds

The data obtained for cumulus *Ac* and *Cc* allowed us to assume the following. First, $dV(r)/dr$ distributions in cumulus are vary stronger than tose in cirrus, and in *Cc* they may vary even within same cloud. Second, particles in *Ac* clouds are somewhat larger (the position of the mode varies within $r = 3 - 5$ μm, while in *Cc* it is about 1.5 – 3 μm), see Fig. 1*c*. Curves *1–3* correspond to the above-described homogeneous field of *Ac* – for similar cases the shape of the distribution and the position of the mode are rather stable, with only the amplitude of the distribution varying. Curves *4–6* correspond to the *Cc* cloud. They were recorded with the interval less than 2 min. One can easily see how particle size decreases with time. It is just the case with a cloud (obviously, liquid-droplet one), that dissipated during the observations. In the cases of two-layer cloudiness of the type *Ci* + *Ac*, the distribution curve (as was noted in Ref. 2) clearly broke into two modes – for small particles of *Ac* and large ice crystals of *Ci*. The positions of the curve's maxima in these cases well corresponded to those for single-layer clouds, what again confirms the stability of the algorithm for inverse problem solution.

Contrails

The main air corridors "supplying" the contrails for our studies were the airways of the Sheremetevo airport (about ten kilometers to the north) and Vnukovo (about three times farther to the south). Therefore, the southern contrails are markedly older than the northern ones, and they are observed more

often in accordance with the high-altitude wind rose. The contrail described in Ref. 2 is the northern one. It is younger (at the early stage of development) than the southern ones observed in the fall of 1996. Including the data from Ref. 2, we have only ten records of the contrails, therefore our conclusions can only be considered as tentative. Young contrails (~ 10 – 15 min) consist of two fractions of particles with the size $r \sim 2 - 3$ and ~ 10 μm, and the first fraction gradually transforms into the second one with time. In the older southern contrails, the first mode (curve *1*, Fig. 1*d*) can be followed up only in one case. In other cases, no small particles were detected. The mode of the largest particles ($r \sim 20 - 30$ μm) apparently belongs, in part, to cirrus clouds, against the background of which the contrails were observed. The position of the maximum of the main mode in contrails varies in a wider range than in cirrus, while particles themselves are significantly smaller. The contrails look like the formations combining the features of cirrus and cirrocumulus clouds.

CONCLUSIONS

The main results of this paper can be formulated as follows:

1. In cirrus, the position of maximum ($r \approx 25$ μm) of the main mode of the particle size distribution is independent of the optical depth and the cloud subtype. The size distribution is narrow: $\Delta r / r_{max} \sim 0.3 - 0.4$. Particles from this size range give the main contribution into the total volume V_Σ and the optical depth τ of a cloud.

2. All over the obtained data array, the effective radius of particles is estimated as $R_{ef} \approx 35$. The optical depth and the total volume of particles are related linearly: $V_\Sigma = 16\tau$ (the volume is in units of cm^3/m^2).

3. The parameter defining the main characteristics of clouds of the *Ci* type is the content N of particles of the main mode in the column. It is possible that it is the geometrical thickness of a cloud.

4. Cirrocumulus clouds *Cc* contain the smallest droplets – the radius of particles of the main mode is $r = 1.5–3$ μm. Variations of the distribution with the characteristic time of several minutes are most often observed just in these clouds. In the vast even altocumulus, *Ac*, fields, the distributions are sufficiently stable in time (tens of minutes) and varying only in amplitude. The position of the mode's maximum varies within $r = 3–5$ μm for different cases.

5. In contrails, the particle size-distribution depends on the contrail age – in young contrails ($t \approx 15$ min) the function $dV(r)/dr$ has two modes with the maxima at $r = 3$ and $8 - 15$ μm. With time the first fraction transforms into the second one, and it may be completely absent in old contrails. The contrails combine the properties of the clouds of *Ci*, *Cc*, and *Ac* types.

REFERENCES

1. A.A. Isakov, Izv. Ross. Akad. Nauk, Fiz. Atmos. Okeana **30**, No. 2, 241–245 (1994).
2. A.A. Isakov, Atmos. Oceanic Opt. **10**, No. 7, 722–733 (1997).
3. A.Kh. Khrgian and N.I. Novozhilov, eds., *Album of Clouds* (Gidrometeoizdat, Leningrad, 1978), 268 pp.
4. A.P. Gritsenko and G.D. Petrov, Opt. Spektrosk. **46**, No. 2, 346–349 (1979).
5. V.F. Belov, A.G. Borovoi, N.I. Vagin, and S.N. Volkov, Izv. Akad. Nauk SSSR, Fiz. Atmos. Okeana **20**, No. 3, 323–327 (1984).
6. T.M. Abakumova, P.P. Anikin, and Yu.V. Glushchenko, in: *Radiation Properties of Cirrus Clouds*, e .l . Feigelson, ed. (Nauka, Moscow, 1989), 224 pp.
7. J.F. Gayet, G. Febvre, G. Brogniez, H. Chepfer, W. Renger, and P. Wendling, J. Atmos. Sci. **53**, No. 1, 126–138 (1996).